



COLOR HOLOGRAPHIC INTERFEROMETRY (FROM HOLOGRAPHIC PLATES TO DIGITAL HOLOGRAPHY)

J.M. DESSE^{1,c}, P. PICART²

¹ONERA, The French Aerospace Lab, Lille, F-59045, France

²LAUM-ENSIM, Laboratoire d'Acoustique du Maine, Le MANS, 72085, France

^cCorresponding author: Tel.: +3332496940; Fax: +33320498527; Email: jean-michel.desse@onera.fr

KEYWORDS:

Main subjects: flow visualization

Fluid: unsteady flows, flows with shocks

Visualization method(s): holographic interferometry

Other keywords: image processing, color holography

ABSTRACT: A comparison of optical non invasive techniques using panchromatic holographic plates and digital holography for analyzing unsteady wake flows is detailed. Few years ago, ONERA developed optical methods based on real-time three-wavelength holographic interferometry using transmission and reflection holographic plates. These techniques combine the advantages of differential interferometry with those of monochromatic holographic interferometry. Real-time three-color transmission holographic interferometer is first described in which transmission holograms are used. It is shown that diffraction efficiency of holograms just reaches ten or twenty percents, that which limits the quality and the contrast of interferences fringes.

Then, compact real-time three-color reflection holographic interferometer was developed where reflection panchromatic silver-halide holographic plates are used to simultaneously record three reference holograms. Best results are obtained when the diffraction efficiency of holographic plate reaches 50% for the three used wavelengths. This optical setup was applied for analyzing 2D unsteady wake flow around a circular cylinder at subsonic Mach number. To avoid problems in gelatin shrinkage due to the hologram treatment, ONERA is developing digital color holographic interferometry. Here, three interference micro fringes are generated in the observed field. A 3CCD sensor records reference (without flow) and measurement (with flow) interferograms and the phase and amplitude maps are computed by direct and inverse 2D Fast Fourier Transforms in delayed time. Results can be directly compared to those obtained in color holographic interferometry using panchromatic plates. An example is given here on the same test case where color interferences fringes can be compared.

1. Introduction

In monochromatic interferometry, it is well known that the classical interference pattern is represented by a succession of dark and bright red fringes. Unfortunately, the zero order of interferences fringes can never be identified and it is one of the major difficulties with interferences fringes in monochromatic light. Sometimes, it is not possible to follow the displacement of the fringes through a shock wave, for example, or to count the fringe number in a complex flow. When the light source is a continuous source, the interference pattern is a colored fringe pattern in a sequence approximately matching Newton's color scale. This fringes diagram exhibits a unique white fringe, visualizing the zero order of interference and it allows one to measure very small path differences. But, when the path difference is greater than three or four microns, the colors can no longer be separated and the larger path differences cannot be correctly measured. If three different wavelengths are used as luminous light source of interferometer, the fringes obtained show that the disadvantages of the two others sources have disappeared. The zero order is always identifiable and the colors always remain distinguishable for the small and the large path differences. The interference pattern also presents the following peculiarity: while the white fringe is not visible on the interferogram, the sequence of three successive colors in the diagram is unique [1].

Until recent years, experiments in holographic interferometry were performed with a single laser, i.e., they were monochromatic. Most experiments found in the literature relate to transmission holograms and few experiments



have been performed to date using holographic interferometry with reflected white light. It should be said that, in monochromatic mode, experiments in reflected white-light holography have little advantage over holographic interferometry in transmitted light. Some publications mention the use of three-wavelength differential interferometry and holographic interferometry by reflection and all show that the essential advantage of color is that the achromatic fringe can be located in the observed field.

It is for this reason that ONERA decided to develop real-time true color holographic interferometry using three primary wavelengths (red, green, blue lines) to record the interference between the three object beams and the three reference beams simultaneously on a single reference hologram.

2. Real-time color transmission holographic interferometry

The optical setup has been developed around ONERA's wind tunnel at Lille centre [2]. For reference, this wind tunnel is equipped with a 2D test section 200 mm high and 42 mm wide. The Mach number can be varied from 0.3 to 1.1. The flow studied was the unsteady flow downstream of a cylinder 20 mm in diameter D placed crosswise in the test section.

2.1 Optical setup around the wind tunnel

The optical setup is shown in Fig. 1. The beam power as it leaves the laser is 1.80 W when the etalon is set perpendicular to the laser beam axis and 1.20 W when it is tilted. The polarization of the three beams rotates 90° at the exit from the acousto-optic modulator, so that the polarization vectors lie parallel to the reflecting surfaces of the mirrors. This arrangement makes it possible to have beams of the same polarization interfere on the hologram. The three wavelengths downstream of the acousto-optic cell are split into a reference beam and object beam by a beam splitter cube. A right angle prism is used to adjust the reference and object path lengths on the hologram. A spatial filter is used to expand the beam for its passage through the test section. A pair of achromatic lenses converts the beam into parallel light in the test section and then focuses it on the hologram. The reference beam passes over the test section, and then another achromatic lens is used to illuminate the hologram with a parallel light beam. For reference, the object beam diameter is 40 mm at the hologram and that of the reference beam is 60 mm. At the acousto-optic cell, the power of the three light waves is practically the same (of the order of 70 mW per channel). The beam splitter cube distributes 85% of this power to the reference path and 15% to the measurement path.

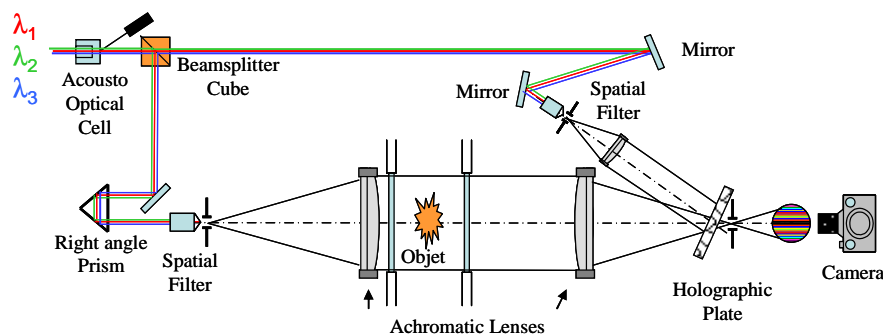


Fig. 1. Optical setup implemented around the wind tunnel

At the hologram, one measures $250 \mu\text{W}/\text{cm}^2$ in the red and blue lines and $280 \mu\text{W}/\text{cm}^2$ in the green line for the reference beam, while the object beam powers are $30 \mu\text{W}/\text{cm}^2$ in the red line and $40 \mu\text{W}/\text{cm}^2$ in the green and blue lines. These proportions can be used to obtain a perfect balance among the powers of the three waves diffracted by the hologram when re-positioning it, and the three live waves. For reference, the hologram diffracts $70 \mu\text{W}/\text{cm}^2$ in the red line, $65 \mu\text{W}/\text{cm}^2$ in the green line, and $90 \mu\text{W}/\text{cm}^2$ in the blue line. The first exposure lasts 2 s. The holograms are then subjected to treatments to harden the gel, develop it, and bleach it. When the hologram is put back in place, the light power at the camera entrance is $1.5 \cdot 10^{-3} \text{ W}$ at the focal point, which is sufficient to record interferograms at an ultra-high speed of 35,000 frames per second with an exposure time of 750 ns per shot.



2.2 Results and analysis of interferograms at Mach 0.37

Fig.2 gives a sequence of six interferograms of the flow around the cylinder at Mach 0.37. The time interval between each picture is 100 μ s. One can see that each vortex is represented by concentric rings of different colors where each color represents an isochoric line. The vortex formation and dissipation phases can be seen very clearly while the fringes oscillate between the upper and lower surfaces of the cylinder. Several types of measurements were made by analyzing a sequence of some 100 interferograms. First, the vortex centre defined by the centre of the concentric rings was located in space for each interferogram, which made it possible to determine the mean paths for the vortices issuing from the upper and lower surfaces. The results of this are shown in Fig. 2b. The “o” symbols represent the positions of the vortex centers from the upper surface, and the “•” symbols those of the lower surface. Remarkably, the two paths exhibit a horizontal symmetry about the $x = 0$ axis passing through the cylinder centre. One may also point out that even at $x/D = 4$ downstream of the cylinder, the upper and lower vortex paths do not come together and line up.

Lastly, the colors of each interferogram were analyzed using the “MIDI” software, which models the light intensity and experimental interference fringe colors as a function of the path difference. The gas density measured under free stream conditions is the same as that measured at the outer flow of the wake (measured in the vicinity of the wind tunnel’s upper and lower walls).

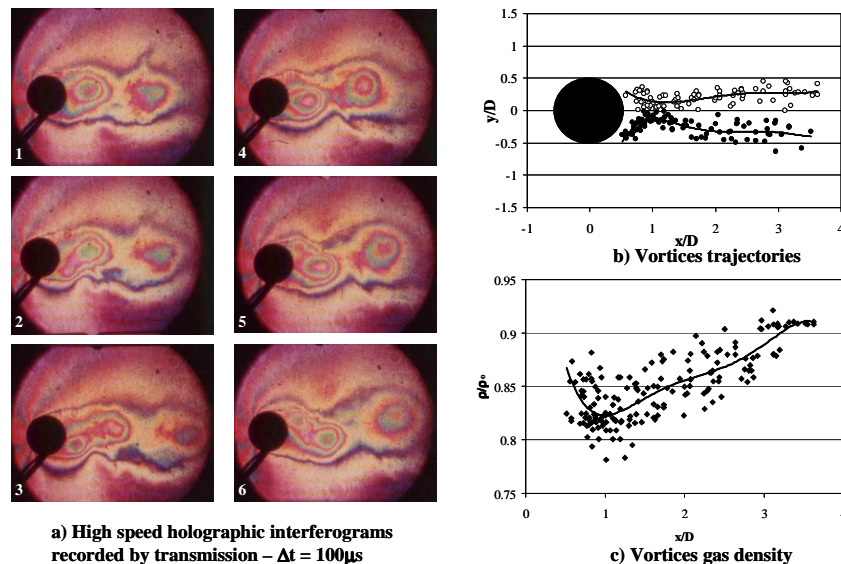


Fig. 2. Unsteady wake flow around the cylinder -Results and analysis – Mach 0.37

3. Real-time color reflection holographic interferometry

Since transmission holograms are used, the diffraction efficiency of holograms just reaches between 10% and 20%, which limits the quality and the contrast of interferences fringes. On the other hand, if reflection holograms are used, the theoretical diffraction efficiency can reach 100% with a monochromatic light. The development of real-time true color reflection holographic interferometry also offers two important advantages. The first one concerns the analysis of the three-dimensional (3D) flows and the second one lies in the comparison with digital colour holographic interferometry. In fact, ONERA is looking towards analyzing unsteady 3D flows, and the optical setup to be designed must be based on several crossings of the flow along different view angles. It is very evident that classical optical setup based on monochromatic holographic interferometry defined in section 4, for instance, for analyzing two-dimensional (2D) flows, cannot be reproduced three or four times. Moreover, as the optical path differences to be measured are smaller in 3D flows than in the 2D case, it is preferable that each optical ray crosses the phenomena twice in order to increase the sensitivity. Also, to simplify the setup, all the optical pieces have to be located on the same side of the wind tunnel, except the flat mirror which reflects the light rays back into the test section.



3.1 Description of optical bench

The optical setup could be named “Denisyuk” because it uses a holographic plate in a classical Lippmann-Denisyuk in-line experiment. To obtain a simple setup, all the optical pieces are located on the same side of the wind tunnel, except the flat mirror which reflects the light rays back into the test section. Due to these considerations, the optical setup based on real-time color reflection holographic interferometry has been designed [3]. It is presented in Fig. 3.

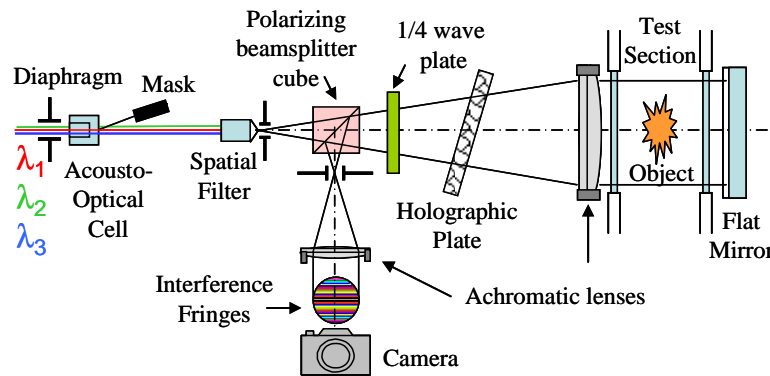


Fig. 3. Real-time three-color reflection holographic interferometer

Here, the light source used behind the interferometer is constituted with three different lasers. An argon-krypton laser delivers the red line ($\lambda_1 = 647$ nm), and a green line ($\lambda_2 = 532$ nm) and a blue line ($\lambda_3 = 457$ nm) are given by two diode pumped solid state lasers. A spatial filter is just located at the focal point of the large achromatic lens which is set in the front of the test section so that the object under analysis is crossed by a parallel light beam of 200 mm in diameter. A flat mirror located just behind the test section returns the three beams on the hologram inserted between the quarter wave plate and the large achromatic lens. The hologram is illuminated on the two sides by the three collimated reference and measurement waves which are formed by the convergent and divergent achromatic and lenses. This arrangement allows one to easily obtain before the test a uniform background color (infinite fringes) or narrowed fringes (finite fringes). In this setup, a polarizing beam splitter cube is inserted between the spatial filter and the quarter wave plate which transforms the waves polarization twice (from P parallel to circular and from circular to S parallel) so that, when the rays are returning, the beam splitter cube returns the rays towards the camera. A diaphragm is placed in the focal plane just in front of the camera in order to filter out any parasitic interference. The interferences fringes produced by the phenomenon under analysis can be directly recorded using high speed camera. Here, the camera used is a CORDIN 350 Dynafax. The size of each recording is 10x8 mm² and the pictures are taken in a staggered pattern on a 35mm film. High sensitivity (800/1600 ASA) daylight reversible colour films are suitable.

First, the holographic plate is simultaneously illuminated with the three wavelengths. The panchromatic hologram records simultaneously the three sets of interference fringes produced by the three incident waves and the three waves reflected by the flat mirror (first exposure). Then the hologram is developed and it is reset in the optical bench at the same location. At the second exposure, if the diffraction efficiency of the holographic plate is near to 50% for the three lines, 50% of the light is reflected by the hologram and 50% crosses the holographic plate. If a mask is inserted in the front of the test section, one can observe on the screen the three images diffracted by the plate. This operation allows for verifying the quality of the holograms diffracted. When the mask is moved, 50% of the light crosses the test section twice and interferes in real-time with the three references waves. Interference fringes are not localized because they can be observed from the holographic plate to the camera. If no disturbances exist in the test section, a uniform background color is obtained in the camera. If variation in refractive index exists in the test section, color fringes will be seen on the screen. As the luminous intensities of reference and measurement waves are basically equal, the contrast of color interferences fringes will be maximum.

This optical setup is very simple but it presents some advantage and some inconvenience. The advantage lies in the small number of optical pieces which are used. A main inconvenience resides in the fact that it is not possible to



adjust the diffraction efficiency of the holographic plate. It is only fixed by the chemical treatment and it is a function of gelatin thickness.

Finally, the three interference fringe patterns will exist and can be recorded if the coherence length of the three wavelengths is more than twice the distance between the holographic plate and the flat mirror located just behind the test section. Compared to the setup of transmission holographic interferometry, here it is not possible to adjust the length between the reference and measurement rays.

3.2 Wind tunnel implementation of optical technique

The real-time color reflection holographic interferometer has been implemented in the ONERA transonic wind tunnel for analyzing the same unsteady wake flow around the cylinder. Here, the infinite Mach number was fixed at 0.45. The time interval between two successive frames is 117 μ s. The time exposure (750 ns) of each interferogram is given by a small window size inside the camera and the number of recorded interferograms is about 220. Several movies have been recorded with uniform background color (infinite fringes), circular and narrowed fringes (finite fringes). As the optical setup is very sensitive to external vibrations, the uniform background color is difficult to adjust when the wind tunnel is running, but the fringe formation can be observed on the hologram surface so that it is possible to adjust the uniform background color with the wind tunnel operating. Fig. 4 shows three of twelve interferograms covering about a period of the vortex street. They are recorded in infinite fringes. The interferogram colors are well saturated and of higher contrast than those obtained in previous experiments performed with transmission holograms.

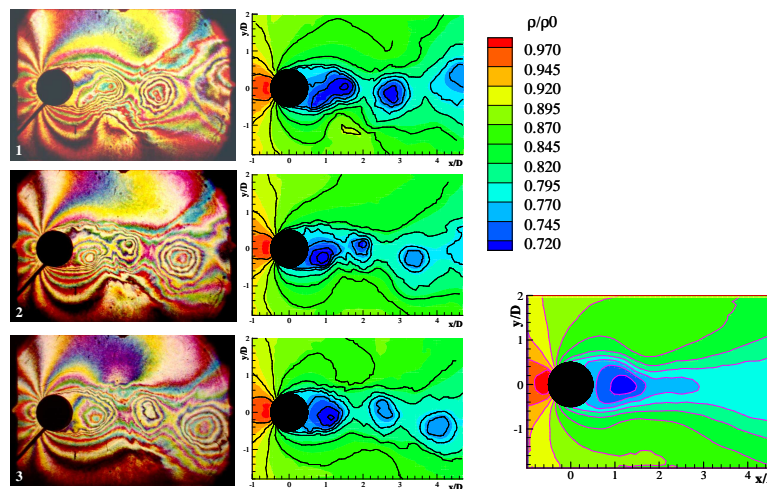


Fig. 4. Interferogram analysis : instantaneous and average gas density field – $\Delta t = 117\mu$ s

It is very easy to follow the vortices emitted from the upper and lower side. For instance, if one looks at the colors coming out in the vortex cores, one can easily see that the first vortex emitted from the upper side enters a formation phase where the gas density decreases in the vortex centre. A second phase of dissipation is observed looking at the last vortex leaving the observed field. Finally, as with transmission holographic interferometry, each color represents a value of the gas density. In analysis, the gas density field was referred to ρ_0 , the stagnation gas density. One can see that the instantaneous gas density varies from 0.70 to 0.98. The average gas density in the field has been calculated from twelve successive interferograms. The interferogram number is not very significant, but the obtained field is already symmetrical enough and the gas density varies from 0.72 to 0.97. Finally, if the color scale of interference pattern is very well known to the user, the image of interferograms is sufficient to correctly evaluate the evolution of the gas density field.



4. Digital color holographic interferometry

The fast development of technology, such as high resolution sensors, various DPSS lasers with large coherence, data post processing and computation power provide now opportunities to conceive new optical methods capable of simultaneous full field measurements with high spatial and temporal resolutions and giving absolute data. Digital holography with matrix sensors appeared in the last decade with cheap high resolution CCD cameras and the increasing power of computers. As regards these works, ONERA and LAUM decided to join their respective competences acquired in the past in order to develop adaptable and new optical imaging methods, firstly having properties such as full field imaging with high spatial and temporal resolutions, secondly giving absolute data after post processing and finally giving dynamic three dimensional measurements. These non-invasive optical methods are based on digital color holography.

4.1 Digital Michelson holographic interferometer

The assembly shown in Fig. 5a is very simple. It is like a conventional Michelson interferometer in which a beam splitter cube is inserted between the spatial filter and the test section [4]. The spatial filter is placed at the focal point of the achromatic lens so that the test section is illuminated with a parallel light beam as in previous optical setups. 50% of the light is reflected from the concave spherical mirror to form the three reference beams and 50% of light passes through the test section to form the three measurement waves. The flat mirror, placed just behind the test section, returns the beams towards the beam splitter. 25% of light is focused on the diaphragm which is placed in front of the camera lens. So, 25% of the reference beam intensities are focused in the same diaphragm by the concave mirror.

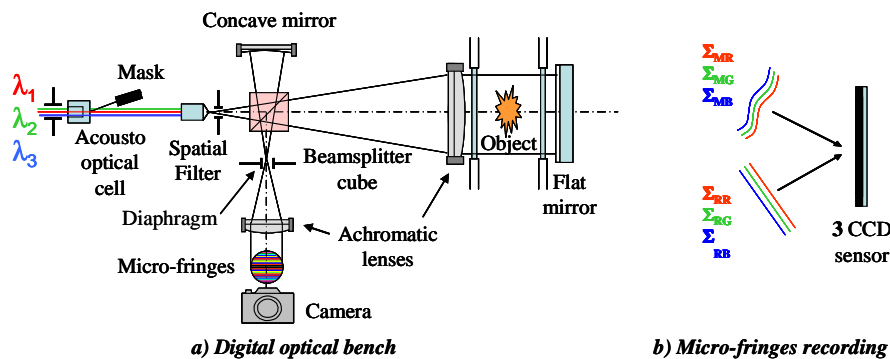


Fig. 5. Digital color holographic interferometer – Formation of spatial carrier frequencies

4.2 Results obtained in subsonic wake flows

Again, near wake flow downstream from a circular cylinder has been studied at Mach 0.45. Here, one used a ORCA-3CCD Hamamatsu camera with 3 chips of 1344x1024 pixels, 6.45 μm x 6.45 μm in size. The framing rate is 9 f/s and the filters of RGB camera are very narrowband and centered on the three laser wavelengths. As the framing rate is very slow compared to the frequency of the vortex street, a transducer has been implemented in the cylinder at an azimuth of 90° (perpendicular to the flow axis) in order to synchronize the interferogram recording with the signal of the unsteady pressure measurement. The cycle of the vortex street was decomposed in eight different instants shifted by 76 μs and at each instant, five interferograms were recorded from several cycles to average the unsteady maps. First, Fig. 6 shows two micro fringes images recorded with and without the flow in order to constitute reference and object interferograms. It can be seen in the zoomed image that micro-fringes are deformed by the shear layer of the upper side.

The three Fourier transforms are calculated from each image in order to reconstruct the phase maps with the +1 order (the zero order and the -1 order are filtered). An example of reference and measurement spectra is given in Fig. 7 for the green line. One can see that the spectrum only exhibits a spot corresponding to the green spatial carrier frequency. No parasitic frequencies due to the blue and red lines are found. By subtracting the reference phase maps



from the measurement phase maps, one obtains the modulo 2π phase difference maps. After unwrapping, it possible to compute the refractive index maps and the gas density field assuming the Gladstone-Dale relation.

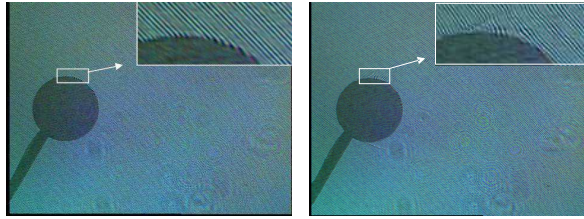


Fig. 6. Micro-fringes recording for the reference and object images

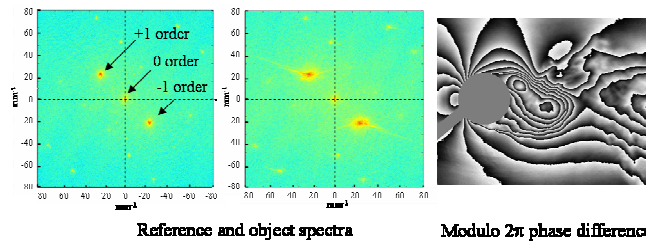


Fig. 7. FFT reference and object spectra and difference phase map for the green line

Color interferences fringes and gas density field are shown in Fig. 8 for the first three images of one cycle of the vortex street.

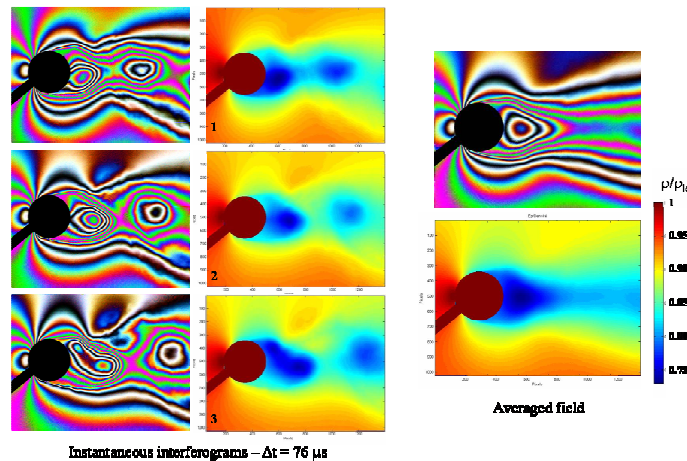


Fig. 8. Evolution of color interference fringes and gas density field – Mach 0.45

The intensity of the interference fringes is computed on the three channels R, G, B from the phase maps with following the following relationship : $I_l = A_l (I + \cos(\Delta\phi_\lambda))$. The gas density measured to the cylinder nose is particular as the gas density is equal to the stagnation gas density though the position of the vortex street, that means the color found at this point has to be the same on each interferogram. Here, the intensity of color interferences fringes is computed by imposing the white color ($\delta = 0 \mu\text{m}$) on each interferogram. Note this shifting is only made possible by the use of color in the experiments. The time evolution of the gas density fields shows that the gas density decreases to 73% of ρ_{i0} in the vortex core. Then, the averaged field of one cycle is calculated by averaging the 8 maps of instantaneous gas density field.

4.3 Comparison between holographic plate and digital holograms

As regards previous results obtained, silver-halide plate and digital holographic interferometry can be compared. The only possibility to compare plate and digital interferograms is to compare the interferograms displaying the interference fringes. Indeed, the technique of holographic interferometry in real time using panchromatic plates



directly displays the color density variations of the flow. It's a light intensity information that is obtained. With digital holography, the three monochromatic intensity maps are superimposed to obtain a color map of the intensity of the interference fringes. This map can then be compared to that obtained using the reflection holographic plates. After locating an interferogram recorded at a phase very similar to that of digital interferogram, Fig. 9 shows that the correspondence is very good.

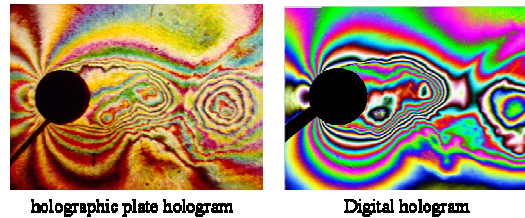


Fig. 9. Comparison between image and digital interferogram

5. Conclusion

The possibilities of image and digital color holographic interferometry have been demonstrated. Color holographic interferometry using panchromatic plates will continue to be used due to the high resolution of holographic plates. In near future, digital three-wavelength holographic interferometry seems the best candidate to characterize the future complex flows. Although CCD resolution and size are not as good as that of holographic plates, the digital approach is more accessible and versatile since the time for the hologram processing is greatly reduced and the processing is purely numerical. On the other hand, the value of using color has been demonstrated as the zero order fringe can be easily determined and the variation in the background color due to disturbances can be quantified. The limitations of the digital method seem to lie in the wide spectral sensitivity of the sensor which produces light diffusion in each monochromatic hologram. Work is currently in progress for removing the color diffusion using a segmentation approach.

Success in this strategy will allow increasing the spatial resolution in the reconstructed object. Future work will focus on the extension of the proposed technique for analyzing the high density gradients and 3D unsteady wake flows. At present, a specific setup of digital holographic interferometry has been defined in a single sight direction, and the aim will be to reproduce the same optical setup along several sight directions, each shifted by a given angle. It is obvious that the optical setup can be reproduced no more than three or four times. But the lack of sight directions should be compensated by high tomographic interferogram resolution for the reconstruction of the 3D gas density field.

Acknowledgments

The author thanks Jean-Louis Tribillon, retired, from Délégation Générale à l'Armement and Félix Albe, retired, from Institut Franco-Allemand de Recherches de Saint-Louis for their collaboration for developing the transmission and reflection holographic interferometers. A great thank also to Professor Pascal Picart from Laboratoire d'Acoustique du Maine for the implementation of digital holographic interferometry in ONERA.

References

1. Desse J.M. *Three-color differential interferometry*. Appl. Opt. 1997, **36** (28), p. 7150.
1. Desse J.M et al. *Real-time color holographic interferometry*. Appl. Opt. 2002, **42** (25), p. 5326.
2. Desse J.M. et al. *Real-time three-color reflection holographic interferometry*. Appl. Opt. 2009, **48** (36), p. 6870.
3. Desse J.M. et al. *Digital color holography applied to fluid and structural mechanics*. Opt. Las. Eng. 2012, **50**, p. 18.